JACOBS PUBLISHERS

OPEN ACCESS

Jacobs Journal of Forensic Science

Perspectives

FIB/SEM Haemotaphonomy: Red Blood Cells Identification in Unprepared Samples of Forensic Interest

Marziale Milani[1], Roberta Curia[1,2], Claudio Savoia[3]

[1]*Department of Materials Science – University of Milano-Bicocca, via Cozzi 55, 20125 Milan, Italy.*

[2]*Department of Biotechnology and Biosciences – University of Milano-Bicocca, piazza della Scienza 2, 20125 Milan, Italy.*

[3]*ST Microelectronics, Via Olivetti 2, 20864 Agrate Brianza (MB), Italy.*

**Corresponding author: Prof. Marziale Milani, Department of Materials Science – University of Milano-Bicocca, via Cozzi 55, 20125 Milan, Italy, Tel: +390264485175; Email: marziale.milani@mater.unimib.it*

Received: 05-15-2015

Accepted: 05-21-2015

Published: 05-30-2015

Abstract

In our work we analyze through electron microscopy, based on FIB/SEM (Focused Ion Beam/Scanning Electron Microscope), the haemotaphonomy of different blood samples set on diverse substrates. Our aim is to show new electron and ion microscopy techniques through which it is possible to observe non-treated and non-prepared blood samples. This approach can be of use in activities where samples are nor treated and at times neither well conserved, as in the archeological field, and in forensic researches where samples ought not to be contaminated and need to be preserved in the event of further counter analyses.

Keywords: Haemotaphonomy; Red Blood Cells; FIB/SEM; Electron Microscopy; Ion Microscopy; Cell Morphology; Forensic Sciences.

Abbreviations

RBC: Red Blood Cell;

FIB/SEM: Focused Ion Beam/Scanning Electron Microscope

HFW: Horizontal Field Width

Introduction

Blood is a connective tissue made up of plasma and a corpuscular part, formed by erythrocytes, leucocytes and thrombocytes. Red blood cells (RBCs) are the most common type of blood cells, in each cubic millimeter of blood there are 4-6 millions of erythrocytes. RBCs in mammalians are anucleated cells, shaped as biconcave discs, with a diameter of about 6-8 µm, and an average life of 120 days [1].

In this work we analyzed through FIB/SEM (Focused Ion Beam/Scanning Electron Microscope) microscopy [2] the haemotaphonomy [3] of different blood samples (heparinized and centrifuged blood from the morgue or fresh peripheral blood from alive donors), laid on several supports (silicon and metal/plastic stands, paper filter, cotton fiber, and copper wire), as to mimic the bloodstains that a forensic laboratory has currently to analyze. The term haemotaphonomy, coined by Policarp Hortolà, refers to "the study of bloodstains, and especially of the changes in appearance

and size of the cellular components, as well as the characteristics of their cell position and appearance in function of the superficial topography and composition of the substrate" [3]. The use of a variety of supports can be helpful in order to draw up a database that can be consulted for data retrieval during forensic investigation. It is shown that RBCs can be detected in many cases, this is of relevance since the presence of RBCs in forensic biology is the confirmation of the presence of blood in the smear [4]. Size and shape of RBCs are useful parameters to detect any deviation from normal cells indicating any minor diversity or pathological states. In our analysis it is possible to characterize the RBCs' morphology; cytomorphology can change depending on the different mountings but is anyway stable thanks to the number of cells simultaneously observed that allows a statistical analysis.

The technique we propose can be applied to both treated (chemically prepared and/or conductively coated) and non-treated samples and it can be widely used in archeological and forensic fields where samples need to be preserved to their original state as much as possible, and ought not to be contaminated.

Materials and Methods

The sample from the morgue, provided from the Department of Forensic Medicine of the University of Milan (Italy), was treated with heparin, as an anticoagulant, centrifuged and air dried; the other sample (fresh peripheral blood from alive donors) was not treated but only air dried, in order to minimize the possible contamination and the onset of artifacts due to chemical substances. None of the samples underwent the conductive coating process.

Samples were set on different substrates (with different conductive properties) and analyzed through electron and ion microscopy. Heparinized and centrifuged blood was laid on a silicon stand, a metal/plastic support, a paper filter, and a cotton fiber, whereas fresh peripheral blood was set on a copper wire (1 mm diameter).

The electron microscopy technique used in our investigation is the FIB/SEM one [2]. The FIB/SEM analyses were performed on a Quanta 200 3D (FEI Company, USA) equipped with an ion column and a Tungsten one, a Strata 235 Dual Beam (FEI Company, USA) equipped with an ion column and a FEG (Field Emission Gun), complemented with a Nova NanoSEM 600 (FEI Company, USA) equipped with a FEG.

FIB/SEM analyses can be carried out using two different primary particle beams, in fact FIB/SEM is equipped with two columns or guns (ion and electron). The ion column uses Ga^+ ions (mainly at 30 kV), instead the electron one uses electrons derived either from a Tungsten wire of from a FEG (in the range of 1-30 kV); in both cases secondary electrons, generated by sample-primary beam interactions, are collected by different detectors depending on the specific parameters of the electrons. The two columns give different kinds of images of the same sample not only because of the different interactions of ions and electrons with the sample (penetration depth of the primary beam and particles' mass), but also because of the complex geometry of the whole system dictated by the relative orientation of the ion column, the electron one, the detectors and the sample. FIB/SEM investigation can be operated either in High Vacuum or in Low Vacuum in presence of Nitrogen or water (in order to reduce the charging of the sample) [2].

SEM (High Vacuum) imaging usually requires some sample preparation method. SEM (Low Vacuum) imaging allows to skip some or all the preparation steps, as well as some SEM (High Vacuum) imaging mainly at Low Voltage [2, 5-10]. Our SEM imaging (in the Voltage range of 1-10 kV) does not need standard preparation methods, which heavily affect the sample's properties with the possible appearance of artifacts [11]; it is notable that the ion beam gives good images without any preparation even at 30 kV, notwithstanding the milling/etching effect originated by the high kinetic energy of the ions. Moreover our FIB/SEM imaging is performed in the absence of any sample coating, in fact we observe air dried samples without any further treatment, thus preparation procedures become quicker and simpler.

Finally FIB/SEM technique in our case allows us to better discriminate the RBCs' secondary electrons contribution from that generated by the substrate. Actually the combined use of ion and electron beams permits the investigation of sub-surface regions of the sample at different depths, moreover the milling, operated by the ion beam, can be used to generate sections along planes favorable to the analysis, providing images that give a real 3D analysis [2].

In order to compare different microscopy techniques (optical, electron and ion) and to draw up RBCs statistics in anticipation of a future database, images have been processed with GIMP (available from: www.gimp.org).

Results

Heparinized and centrifuged blood was set on different substrates (a silicon stand, a metal/plastic support, a paper filter, and a cotton fiber); here we provide only the image of the sample on a metal/plastic support (Figure 1).

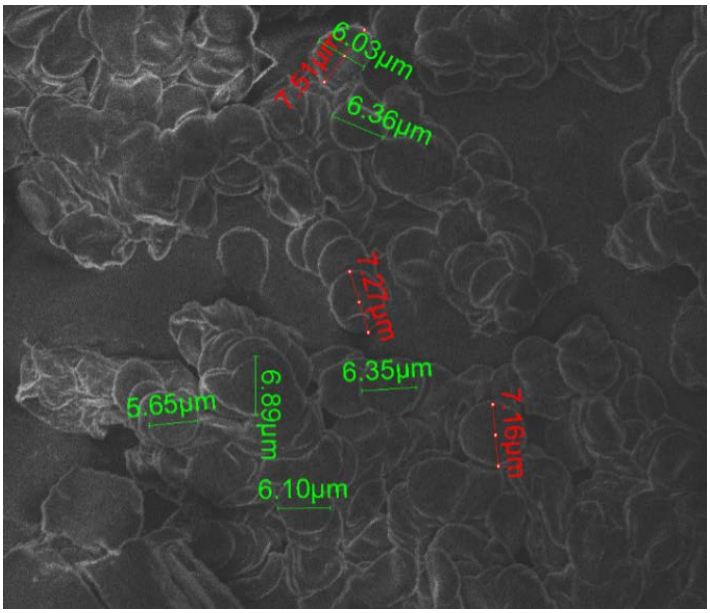

Figure 1. SEM (Nova NanoSEM 600) image of heparinized and centrifuged blood on a metal/plastic support obtained by secondary electrons, at 5 kV electron beam acceleration in High Vacuum. Erythrocytes are clearly visible, some of them form stacks, called rouleaux [12-15]. These aggregates are due to either artifacts or to high concentrations of globulins and fibrinogen. Some of the RBCs' diameters measures are reported. (HFW=79µm).HFW=Horizontal Field Width

Here we present samples of fresh peripheral blood set on a copper wire, seen with both ion (Figures 2a and 2b) and electron microscopy (Figure 3). Depending on the primary particle beam used, the outcome is evidently different. In particular, in the ion image (Figure 2a) the outer part of the cell (torus) seems to be sunken in the sample' surface, whereas the central part of the cell appears closer to the observer. Instead in the electron image (Figure 3) the cell results concave, with its outer part sticking out from the sample and the central one sinking in the sample's surface.

Since in Figure 2a the RBC appears convex, when one would expect the erythrocyte to be a biconcave disc [1], we vertical flipped the ion image (Figure 2a) and analyzed the observers' impressions. In Figure 2b it is shown the same RBC of Figure 2a upside down; here the erythrocyte clearly appears as a concave cell, with a protruding torus and a central part sunken in the sample' surface. The opposite impression that the observer catches looking at the two ion images (Figures 2a and 2b) can be related to neuronal processes that the brain elaborates in order to better detect and recognize objects, as well as to evolution mechanisms that could influence the way the brain processes the images caught by the eye [16].

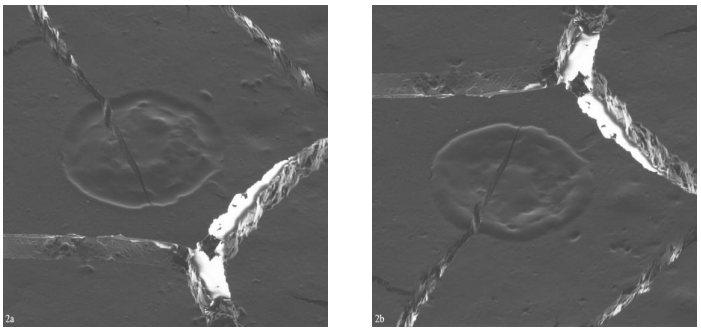

Figure 2. FIB/SEM (Strata 235 Dual Beam) image of a RBC drawn from fresh peripheral blood set on a copper wire, obtained by secondary electrons, at 30 kV ion beam acceleration in High Vacuum. In Figure 2a the erythrocyte appears convex, with the torus sunken in the sample' surface and the central part of the cell emerging towards the observer. Figure 2b shows the same RBC as in Figure 2a vertical flipped: the erythrocyte seen upside down appears concave. (HFW=30.4µm).

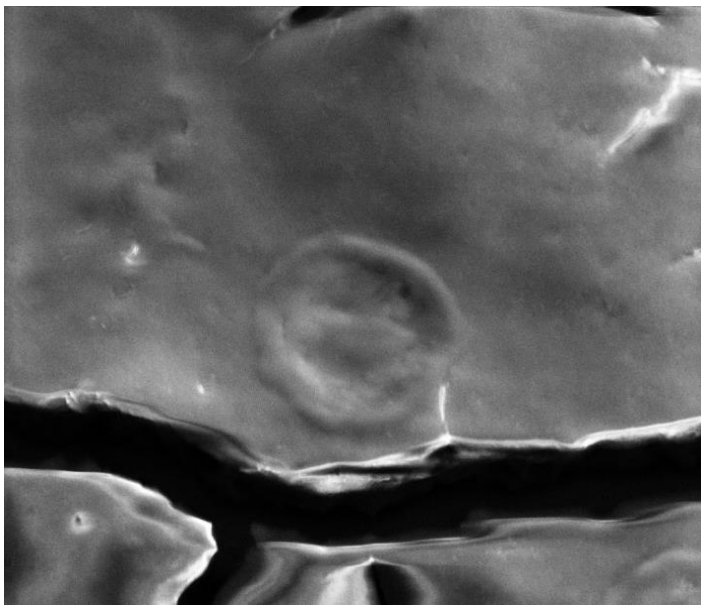

Figure 3. SEM (Nova NanoSEM 600) image of a RBC drawn from fresh peripheral blood set on a copper wire, obtained by secondary electrons, at 10 kV electron beam acceleration in High Vacuum. The RBC seen with the electron beam appears concave, with the torus sticking out from the sample and the central part of the cell sunken in the sample's surface. (HFW=46.5µm).

RBCs seen with the ion beam appear not only convex, but even almost elliptical (Figure 4). This effect, due to the angle of the ion column (52°) compared with that of the electron one, has been well explained by Euclid in his theorem XXXVI: a wheel is seen sometimes as a circle, sometimes as an ellipse. Therefore, setting aside the geometry of the object itself, the ellipse de-

pends more on the perspective from which the observer, in our case the detector, studies the object [17] (Figure 5). Anyway, in electron and ion imaging the problem is really complex and discussions about the so called "mirror effect" are still open [2].

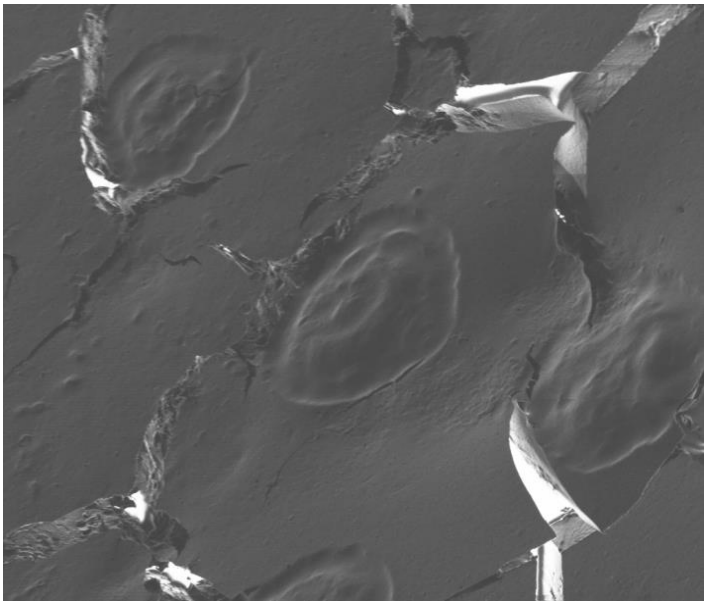

Figure 4. FIB/SEM (Strata 235 Dual Beam) image of fresh peripheral blood set on a copper wire, obtained by secondary electrons, at 30 kV ion beam acceleration in High Vacuum. RBCs show a strong ellipticity, due to the angle of the ion column compared with that of the electron one. (HFW=46.8μm).

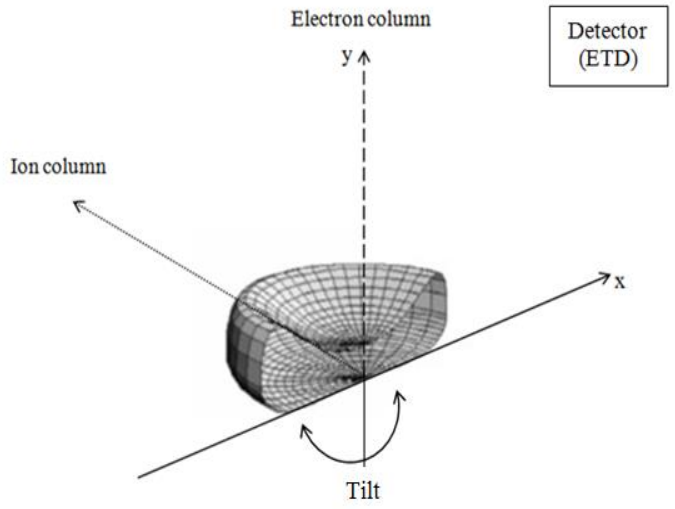

Figure 5. Scheme of the orientation of the ion and electron columns in a FIB/SEM, applied to the Euclid's Optics theorem XXXVI. The electron column is set on the Y axis, perpendicular to the sample (X-Z plane); the ion column is set on the X-Y plane, at a fixed angle (52°) compared with that of the electron column. In this scheme Euclid's wheel has been replaced by a RBC, and the two primary particle beams play the role of the light source in an usual vision process (optics). The main difference between electron and optical (vision) imaging is the fact that electron detectors have an active role on the particles (particles attractors) which can propagate along non-linear (curved) paths, whereas the eye is purely passive (the photons' path is linear). If the path connecting the eye of the observer with the center of the wheel (Y axis) is perpendicular to the plane of the wheel (X-Z plane), the wheel's diameters will result constant under rotation of the wheel in the X-Z plane and the wheel will appear as a circle; if the path is not perpendicular, the wheel's diameters will appear uneven and the wheel will not appear as a circle anymore, but as an ellipse.

In Figures 6 and 7 it is shown a sample of fresh peripheral blood set on a copper wire observed respectively with the ion and the electron beam. As in the previous images (Figures 2a, 2b, 3 and 4) RBCs appear convex when seen with the ion column and concave when they are observed with the electron gun. In Figures 6 and 7 the visible RBCs are bigger than normal erythrocytes, which diameter is 6-8 μm. In fact the diameters of the cells in the sample are longer than 8 μm, therefore more similar to those of megalocytes, mostly oval erythrocytes larger than 8 μm [18].

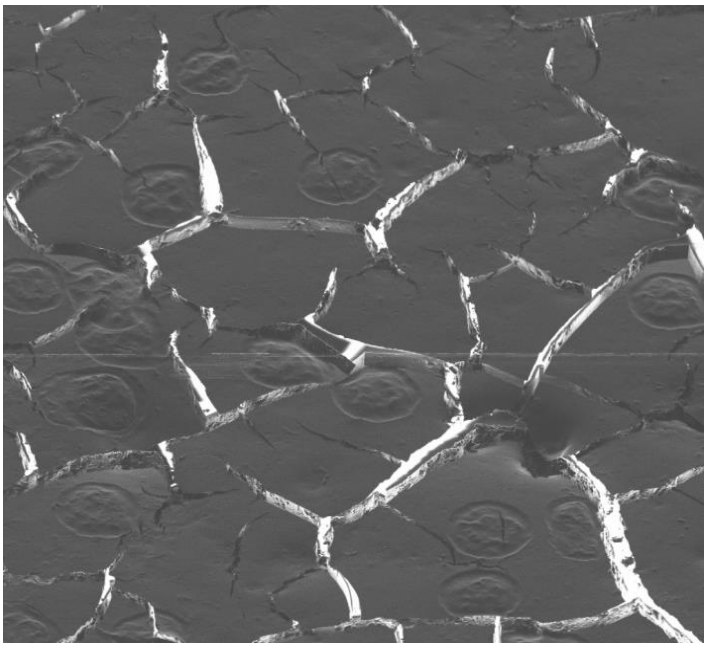

Figure 6. FIB/SEM (Strata 235 Dual Beam) image of fresh peripheral blood set on a copper wire, obtained by secondary electrons, at 30 kV ion beam acceleration in High Vacuum. The cells visible in the sample appear convex, and have an average diameter of 15 μm, bigger than normal erythrocytes, therefore they are classified as megalocytes (large, mostly oval erythrocytes which diameter is longer than 8 μm). (HFW=122μm)

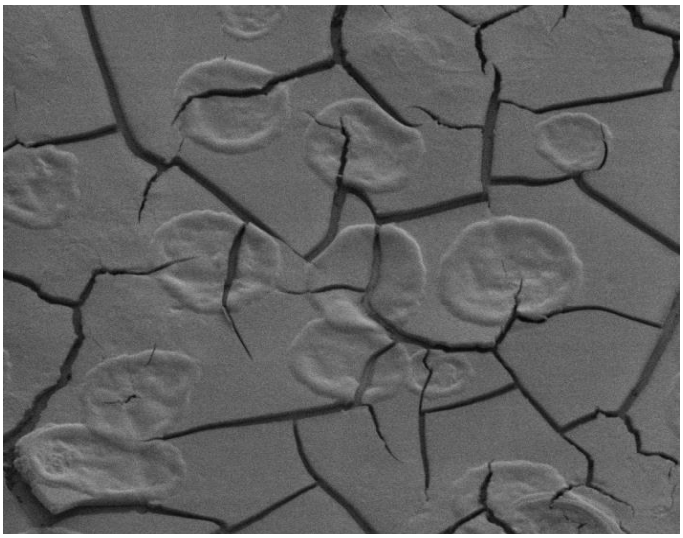

Figure 7. SEM (Nova NanoSEM 600) image of fresh peripheral blood set on a copper wire, obtained by secondary electrons, at 1 kV electron beam acceleration in High Vacuum. The cells visible in the sample appear concave, and have an average diameter of 20.7 μm, bigger than normal erythrocytes, therefore they are classified as megalocytes (large, mostly oval erythrocytes which diameter is longer than 8 μm). (HFW=86.9μm).

As an example in Figure 8 we present an optical image taken from literature in which it is possible to detect normal erythrocytes and megalocytes (arrows), in order to make a comparison between optical, ion (Figure 6), and electron (Figure 7) imaging.

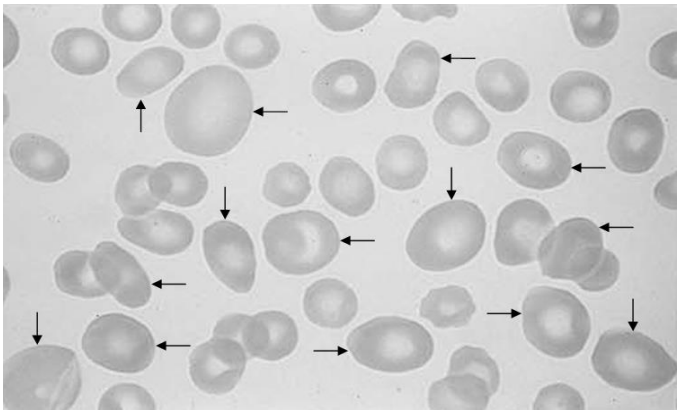

Figure 8. Optical image of RBCs taken from literature. It is possible to see normal erythrocytes together with megalocytes (arrows). Megalocytes appear larger and rather oval than normal erythrocytes. Normal erythrocytes in this image have an average diameter of 6.9 μm; megalocytes have an average diameter of 9.9 μm.

In FIB/SEM imaging the tilt contribution is given not only by the fixed orientation of the electron (perpendicular to the table top, at -90°) and the ion columns (-142°), in fact even the sample plate can be tilted (Fig.5) [2]. In Figures 9 and 10 we present two images of a sample of fresh peripheral blood set on a copper wire observed with the electron beam. In Figure 9 the sample is tilted of 25°, in Fig. 10 it is tilted of 45°. It is evident that the tilt is a powerful tool and its use in the investigation can provide better morphological details. Tilting the sample, it is possible to guide the point of view to the best angle for the observation, in order to get all the information the image can give. Thanks to the tilt of Figure 10, it is possible to measure the width of the outer, thicker part of the RBC (torus).

Figure 9. SEM (Nova NanoSEM 600) image of fresh peripheral blood set on a copper wire, obtained by secondary electrons, at 1 kV electron beam acceleration in High Vacuum. The sample's tilt angle is of 25°. (HFW=86.9μm)

Figure 10. SEM (Nova NanoSEM 600) image of fresh peripheral blood

set on a copper wire, obtained by secondary electrons, at 1 kV electron beam acceleration in High Vacuum. The sample's 45°-tilt angle provides an optimal point of view for the observer to obtain morphological parameters along the 3 axes, as well as the final relative position of the cell embedded or on top of the dried plasma. The megalocyte lays on the surface of the bloodstain, has a 1.3 μm-wide torus and a diameter of 15.6 μm; the thickness of the bloodstain is 7.4 μm. (HFW=20.3μm)

Electron and ion images prove the absence of any hecatocyte or janocyte [4]. Further studies need to be done in order to investigate the meaning of irregular shapes visible in the internal part of RBCs. Eventually, it is important to highlight that electron and ion microscopy techniques provide information regarding the cellular density, useful to deduce the dynamic of the bloodstain's formation.

Discussion

In all the electron and ion images presented in the previous section the only cellular type visible is represented by erythrocytes (both normal and megalocytes). In the next SEM image (Figure 11) we show a sample, the surface of a kidney stone, that underwent the preparation process [19]. It is notable that the preparation fixed not only erythrocytes but even other components, such as collagen fibers.

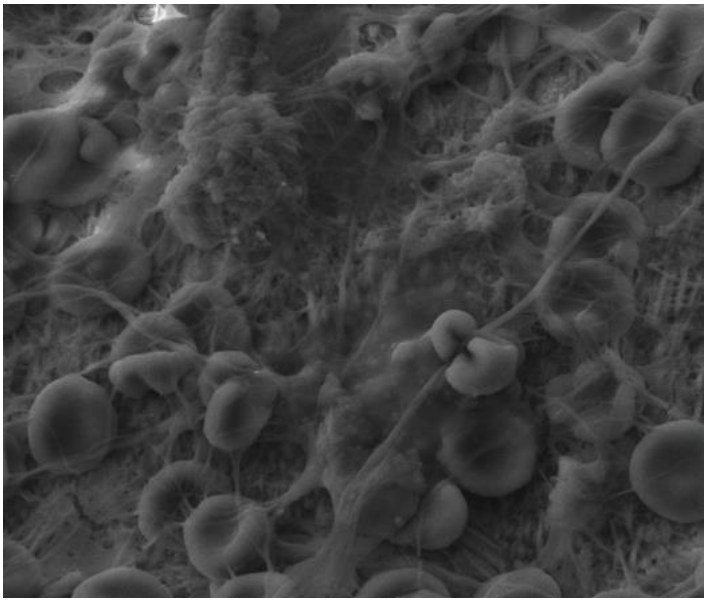

Figure 11. SEM (Quanta 200 3D) image of the surface of a kidney stone, obtained by secondary electrons, at 10 kV electron beam acceleration in High Vacuum. The sample has been prepared as described in Didenko *et al.*, 2014 [19] and in the image it is clearly visible the presence of erythrocytes and collagen fibers. (HFW=49.7μm).

The preparation method fixes all the cells and other components of a sample, and images are very rich in details. On the other hand, the preparation process can heavily affect the sample, creating artifacts and compromising the chemical stability. In forensic sciences, as well as archeological research, it is of primary importance not to contaminate nor spoil the sample [4]. Chemicals, interacting with the sample, could easily modify, erase or cover precious particulars. The feature that makes our work in the forefront of the forensic investigations and in all those sciences where the handling of the sample needs to be reduced to minimal, non-invasive passages is the possibility to examine unprepared samples [5]. In the previous section we presented images of fresh peripheral blood set on a copper wire and only air-dried (Figs. 2a, 2b, 3, 4, 6, 7, 9, 10). As a consequence of the air drying, the copper wire was covered by a thin-layered film, which cracked due to gravity, viscosity and hydrodynamic forces. This fracturing, which sometimes can be seen even in cells, in our images does not affect the informational content thanks to the high number of visible cells.

Electron images were acquired at 1-10 kV beam acceleration, ion images at a beam acceleration of 30 kV. When the sample has a biological nature and did not underwent any coating process, it is better to operate at low voltages [20] in order to reduce damages and the charging of the sample, which leads to poor resolution. It is important to note that prepared and non-prepared cells analyzed in High Vacuum do not present significant alterations neither in the cellular shape, nor in the cellular morphological stability.

Comparing prepared samples (Figure 1) with non-prepared ones (Figures 2a, 2b, 3, 4, 6, 7, 9, 10) it can be affirmed that the cytomorphology is conserved in unprepared samples. Furthermore, analyzing untreated samples with different primary particle beams (ions and electrons), it is possible to appreciate different characteristics. The first difference that the observer catches looking to ion and electron images is that in ion images (Figures 2a, 2b, 4, 6) RBCs appear convex, instead in electron images (Figures 3, 7, 9, 10) erythrocytes appear concave. Most likely this convex/concave ambiguity is correlated to neuronal processes and evolution mechanisms that the brain uses in order to process the 2D images caught by the eye and recognize the objects contained in them [16]; thus this effect seems not related neither to the lack of the preparation process nor to the air drying: in fact vertical flipping the ion image the erythrocyte appears concave (Figures 2a and 2b).

Another characteristic emerging observing ion and electron images is that cells in ion images (Figures 2a, 2b, 4, 6) appear oval, as if flattened along their major axis, instead in electron images (Figures 3, 7, 9, 10) RBCs appear rather circular. This elliptical/circular effect, explained in Euclid's theorem XXXVI, is due to the perspective from which the observer studies the object rather than to the actual geometry of the object itself [17]. It needs to be taken into account that in FIB/SEM microscopy the perspective is influenced by different factors: the angles of the ion and electron columns, the tilt of the sample plate and the orientation of the different detectors (Figure 5) [2].

Electron and ion imaging, compared to the optical microscopy, provide images with better and deeper details of the cells, including information about their morphology along the 3 axes. Here we present two graphs drawn from the analysis of data extracted from electron, ion and optical images. In particular we measured the cells' axes, and compared the major axis' length and the minor axis/major axis ratio, related to other commonly used parameters: area, perimeter and circularity. It has to be noted that the optical image (Figure 8) is taken from literature and the scale was estimated working out the average of the normal erythrocytes' diameters and setting the results equal to 7 μm (the average diameter of a normal RBC).

In Figures 12 and 13 we compared normal RBCs (15 cells) from a prepared sample (Figure 1 - electron image), megalocytes from a non-prepared sample (Figure 6 - ion image - 13 cells; Figure 7 - electron image - 9 cells), and normal erythrocytes (16 cells) and megalocytes (12 cells) from an optical image (Figure 8).

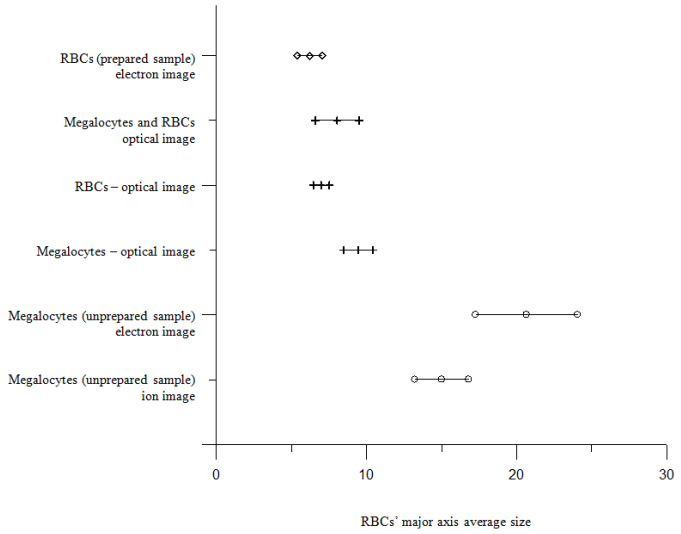

Figure 12. Graph of the RBCs' major axis average length ± standard deviation.

It is notable that the major axis' length of normal erythrocytes seen with SEM is almost in the same range of RBCs seen through optical microscopy. A great discrepancy is observed between megalocytes seen through ion and electron microscopy with those seen through optical imaging (Figure 12).

In Figure 12 it is also reported the major axis average size of RBCs and megalocytes seen through optical microscopy. Since in the sample (Figure 8) the number of erythrocytes and megalocytes is quite homogenous, the statistics are in agreement with the data provided by the single categories.

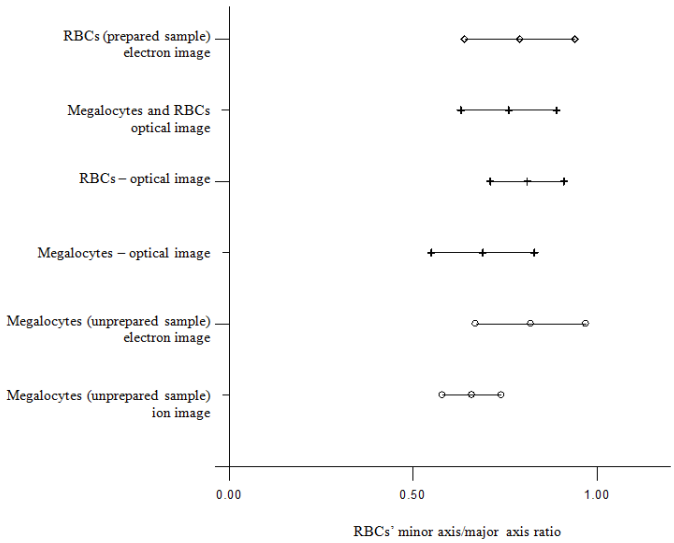

Figure 13. Graph of the RBCs' minor axis/major axis ratio ± standard deviation.

The minor axis/major axis ratio of RBCs gives a result ranging from 0 (non-circular object) to 1 (circular object). All the objects observed have a ratio ranging from 0.50 to 1.00 (Figure 13).

The ratio of megalocytes seen through ion microscopy goes from 0.56 to 0.75, this is due to the fact that in ion images circular objects can appear almost elliptical (Figure 13).

The ratio of megalocytes seen through optical microscopy goes from 0.54 to 0.85 because objects in the sample were rather oval (Figure 13).

Electron, ion and optical imaging give useful results regarding the cells' morphology; the statistical analyses and the creation of a database can give a great contribution to the forensic laboratories for data retrieval during investigation.

Conclusion

This work proves that electron and ion imaging of unprepared samples deposited in an uncontrolled way on various substrates (as those currently analyzed in forensic laboratories) is possible: air drying processes (both in real life and in the FIB/SEM chamber) and High Vacuum do not significantly affect the main features of cells' morphology.

Electron and ion images independently provide in-depth comparable details from which it is possible to extract statistically relevant information useful to go back to the sample's history, to characterize the donor' blood, and to identify him/her.

Concluding, the FIB/SEM technique can be widely used in fo-

rensic sciences and archeological research, since it allows to analyze non-prepared samples, minimizing the chemical processes that could affect the original state of the sample to only physical ones (air drying) and reducing the times for samples' observation. It is finally worthwhile mentioning that all the described procedures can find application in current pathology as a fast tracker of megaloblastic and/or shape-linked pathologies.

References

1. Dean L: Blood Groups and Red Cell Antigens. 2005.
2. Candia Carnevali D, Milani M (Eds.): Proceedings of Summer School 2008 & 2009; Bologna, Italy. Miriam, Società Editrice Esculapio; 2010.
3. Hortolà P. SEM analysis of red blood cells in aged human bloodstains. Forensic Science International. 1992, 40: 139-159.
4. Hortolà P. The "strange" world of bloodstain cells. A brief overview of haemotaphonomy. Problems of Forensic Sciences. 2004, 57: 16-23.
5. Milani M, Drobne D. Focused Ion Beam Manipulation and Ultramicroscopy of Unprepared Cells. Scanning. 2006, 28: 148-154.
6. Milani M, Drobne D, Tatti F. How to study biological samples by FIB/SEM? In Modern Research and Educational Topics in Microscopy. Méndez-Vilas A and Díaz J, Eds. Formatex Research Center. 2007: 787-794.
7. Hortolà P. Using an SEM as an ESEM to Study Minute Human Bloodstains on Stainless Steel. Microscopy and Analysis. 2006, 20(6): 15-17.
8. Hortolà P. Secondary-electron SEM bioimaging of human erythrocytes in bloodstains on high-carbon steel substrate without specimen preparation. Micron. 2008, 39(1): 53-55.
9. Hortolà P. Human bloodstains on biological materials: high-vacuum scanning electron microscope examination using specimens without previous preparation. Microsc Microanal. 2013, 19(2): 415-419.
10. Hortolà P. Haemotaphonomy and the high-vacuum-SEM (re-)examination of bloodstains long after gold coating. Microscopy and Analysis. 2013, 27(1): 21-24.
11. Postek MT, Vladár AE. Does Your SEM Really Tell the Truth? - How Would You Know? Part 1. Scanning. 2013, 35: 355-361.
12. Ponder E. On sedimentation and Rouleaux formation-I. Quarterly Journal of Experimental Physiology. 1925, 235-252.
13. Skalak R, Zarda PR, Jan KM, Chien S. Mechanics of Rouleau formation. Biophys J. 1981, 35(3): 771-781.
14. Samsel RW, Perelson AS. Kinetics of rouleau formation. II. Reversible reactions. Biophys J. 1984, 45(4): 805-824.
15. Del Giudice E, Doglia S, Milani M. Rouleau Formation of Erythrocytes: a Dynamical Model. Journal of Biological Physics. 1985, 13: 57-68.
16. Hubel DH, Freeman WH. Eye, Brain and Vision. Scientific American Library. 1988.
17. Freeland G, Corones A (Eds.) 1543 and all that: image and word, change and continuity in the proto-scientific revolution. 2000.
18. Löffler H, Rastetter J, Haferlach T. Atlas of Clinical Hematology. Springer, USA 2005.
19. Didenko LV, Tolordava ER, Perpanova TS, Shevlyagina NV, Borovaya TG, et al. Electron microscopy investigation of urine stones suggests how to prevent post-operation septic complications in nephrolithiasis. Journal of Applied Medical Sciences. 2014, 3(4): 19-34.
20. Joy DC, Joy CS. Low Voltage Scanning Electron Microscopy. Micron. 1996, 27: 247-263.